

Axial Free Vibration of Euler-Bernoulli Beams via Ritz Method

Ritz Yöntemi ile Euler-Bernoulli Kirişlerinin Eksenel Serbest Titreşimi

Gökhan GÜÇLÜ^{1*}, Uğur KAFKAS²

Abstract

This study used analytical and numerical methods to investigate Euler-Bernoulli beams' free axial vibration behavior with homogeneous and linearly elastic properties. The equations derived within the framework of Hamilton's principle were simplified through a non-dimensionalization approach and the system parameters were consolidated into a single dimensionless stiffness ratio. The analytical solution enabled the computation of natural frequencies by determining the roots of a transcendental equation. The approximate solutions obtained via the Ritz method were compared with the analytical results to assess the method's convergence properties. The results indicate that increasing the number of parameters significantly enhances the agreement of the approximate solutions derived from the Ritz method with the analytical results, thereby validating the method's applicability and effectiveness in structural dynamics analyses.

Keywords: Euler-Bernoulli beam, Axial free vibration, Hamilton's principle, Ritz method.

Öz

Bu çalışmada, homojen ve doğrusal elastik özelliklere sahip Euler-Bernoulli kirişlerinin eksenel serbest titreşim davranışı analitik ve sayısal yöntemler kullanılarak incelenmiştir. Hamilton prensibi çerçevesinde türetilen denklemler boyutsuzlaştırma yaklaşımı ile basitleştirilmiş ve sistem parametreleri tek bir boyutsuz rijitlik oranında birleştirilmiştir. Analitik çözüm, transandantal bir denklemin köklerinin belirlenmesine dayalı olarak doğal frekansların hesaplanmasını sağlarken, Ritz yöntemi ile elde edilen yaklaşık çözümler, yöntemin yakınsama özelliklerini değerlendirmek için analitik sonuçlarla karşılaştırılmıştır. Elde edilen sonuçlar, parametre sayısının artırılmasının Ritz yönteminden elde edilen yaklaşık çözümlerin analitik sonuçlarla uyumunu önemli ölçüde artırdığını ve böylece yöntemin yapısal dinamik analizlere uygulanabilirliğini ve etkinliğini doğruladığını göstermektedir.

Anahtar Kelimeler: Euler-Bernoulli kirişi, Eksenel serbest titreşim, Hamilton prensibi, Ritz yöntemi.

¹Kütahya Dumlupınar University, Department of Civil Engineering, Faculty of Engineering, Kütahya, Türkiye

² Kütahya Dumlupınar University, Department of Construction Technology, Vocational School of Technical Sciences, Kütahya, Türkiye

*Corresponding Author/Sorumlu Yazar: gokhan.guclu@dpu.edu.tr

1. Introduction

As a fundamental pillar of structural dynamics, the study of beam vibrations has wide-ranging applications in mechanical, aerospace, and civil engineering, from skyscraper design to microelectromechanical systems (MEMS) (Gantayat et al., 2024; Rahgozar, 2020). Axial vibration analysis, in particular, provides critical data on natural frequencies and vibration mode shapes—parameters essential for avoiding resonance-induced failures in load-bearing structures (Lee, 2023). Since Euler and Bernoulli first formulated their classical beam theory in the 18th century, engineers have relied on these foundational principles to predict structural behavior under dynamic loading conditions. The Euler-Bernoulli model, which assumes linear elasticity and negligible shear deformation, remains widely adopted for its balance of accuracy and computational tractability in slender beam applications (Yıldırım, 2018).

The inclusion of elastic constraints, such as the spring-terminated boundary examined in this study, reflects practical engineering scenarios where structural components interact with compliant supports—a configuration prevalent in seismic isolation systems and machinery mountings (Kafkas, 2024; Xu and Wang, 2020). Historically, the field has progressed through iterative refinements to governing equations, solution techniques, and experimental validation protocols, with seminal contributions from Timoshenko (Pei, 2024), Rayleigh (Kafkas, 2024; Rao, 2007; Uzun et al., 2021), and more recently, Reddy (2007; 2022) expanding the theoretical framework.

While classical theories are robust for macroscopic structures, recent decades have seen a shift towards analyzing nano- and micro-scale elements where size-dependent effects become significant (Kong et al., 2008; Akgöz and Civalek, 2022). This has led to the development of higher-order continuum theories to capture these phenomena. Foundational work by Reddy (2007) introduced nonlocal theories for the analysis of beams. Subsequent research has applied these and other advanced frameworks, such as modified couple stress theory, to investigate the dynamic behavior of various small-scale structures. Studies have explored the stability and vibration of nanobeams (Civalek et al., 2020), nanorods (Uzun et al., 2023a; Civalek et al., 2022a), nanoplates (Chakraverty and Behera, 2014; Singh and Azam, 2021), and carbon nanotubes (Yaylı, 2015; Uzun et al., 2021). These advanced models are crucial for accurately predicting the behavior of nano-sized beams on elastic foundations (Uzun et al., 2023b; Li et al., 2022) and understanding their complex dynamics.

A significant body of research has focused on applying these diverse higher-order theories to the specific problem of axial (longitudinal) vibration in rods and beams. Models based on modified couple stress theory (Dos Santos and Reddy, 2012), strain gradient elasticity (Akgöz and Civalek, 2014), and surface elasticity (Nazemnezhad and Shokrollahi, 2020) have consistently demonstrated a structural stiffening effect, where natural frequencies increase due to size dependency. Conversely,

theories based on nonlocal principles, such as Eringen's nonlocal elasticity (Civalek et al., 2022b) and peridynamics (Challamel and Zingales, 2025), typically predict a softening effect. More complex models like nonlocal strain gradient theory can capture both hardening and softening behavior (Li et al., 2016), while micropolar (Mirzajani et al., 2018), micromorphic (Nejadsadeghi and Misra, 2021), and micro-inertia-based theories (Soltani et al., 2021) have been used to reveal unique dynamic characteristics, such as wave dispersion influenced by the material's internal microstructure.

The analysis of such vibration problems can be approached through both analytical and numerical methods. Exact solutions typically involve solving characteristic equations derived through the separation of variables (Modak et al., 2023). For spring-supported boundaries, this leads to transcendental equations whose roots correspond to the system's natural frequencies (Elliott and Cammarano, 2024). However, for complex boundary conditions or geometries, closed-form solutions are often intractable, necessitating the use of approximate numerical methods.

Among these, the Ritz method, a widely adopted variational technique, has emerged as a versatile and powerful tool (Ritz, 1909a; 1909b). First applied to beam problems by Warburton (1979), it approximates displacement fields using admissible basis functions, transforming a continuous eigenvalue problem into a discrete matrix formulation. Comparative studies demonstrate its excellent convergence properties relative to exact solutions (Leissa, 2005; Bhat, 1985; 1986). The method's adaptability has been shown in applications to functionally graded materials (Pradhan and Chakraverty, 2013), composite beams (Wang, 1997), and hybrid approaches (Carrera, 1998).

The broad applicability of the Ritz method is evident across the literature. It has been used to examine the buckling of columns with varying cross-sections (Akgöz, 2019) and thin-walled beams (Oguaghamba et al., 2023). Further applications include the analysis of beams on Pasternak foundations (Ranji and Shahbazzabar, 2017), composite Timoshenko and Euler beams (Mazanoglu, 2017), rotating toroidal shells (Senjanović et al., 2018), multi-span continuous beams (Gao et al., 2021), and even complex three-dimensional geometries like elastic ellipsoids (Wu et al., 2023).

This study investigates the axial free vibration characteristics of a homogeneous, linearly elastic Euler-Bernoulli beam with an elastic spring boundary condition, using both analytical and numerical frameworks. The governing equations are derived from Hamilton's principle, incorporating kinetic and potential energy contributions from both the beam and the spring constraint. Through non-dimensionalization, the system's dependence on physical parameters is collapsed into a single dimensionless stiffness ratio, facilitating generalized frequency predictions. The work then establishes an exact solution by finding the roots of a transcendental equation and compares it against an approximate solution obtained via the Ritz method to assess the numerical approach's accuracy.

2. Materials and Methods

2.1. Problem Definition

The beam examined in this study is shown in Figure 1. With the Cartesian coordinate system defined according to the right-hand rule, the positive direction of the y-axis is directed inward on the plane of the page. For points on the axis of the beam, the axial displacement is denoted by $u(x)$, while the vertical displacement is represented by $w(x)$. An elastic spring is located at the left end of the beam, with the spring constant denoted by k . The beam's cross-section is constant, and the material is homogeneous and linearly elastic. The axial free vibration frequencies of the beam will be determined using the Ritz method and compared with the results obtained from the analytical solution.

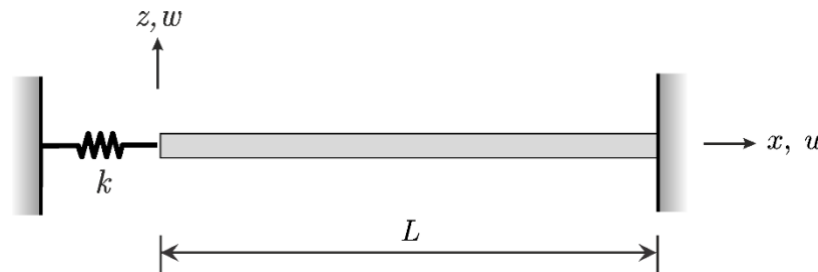


Figure 1. Coordinates, displacement variables and configuration of the beam.

The inclusion of elastic constraints, such as the spring-terminated boundary examined in this study, reflects critical engineering scenarios where structural components interact with compliant supports. For instance, in machinery mountings, flexible supports are used to isolate vibrations and these can be modeled as springs attached to structural beams. Similarly, in seismic design, building columns or bridge piers are often placed on elastomeric bearings that provide a flexible boundary condition against ground motion. In these applications, accurately predicting the axial natural frequencies is essential to prevent resonance-induced failures under operational or environmental loads. Moreover, this model offers significant analytical versatility. By adjusting the spring stiffness, it can represent classical boundary conditions: a stiffness value approaching zero models a free support, while a very large stiffness value approximates a fully clamped support. This makes the spring-supported model a powerful and generalized tool for structural analysis.

2.2. Derivation of the Governing Equation

In Euler-Bernoulli beam theory, the displacement field is expressed by the relations

$$u_1(x, y, z) = u(x) - z \frac{dw}{dx}, u_2 = 0, u_3(x, y, z) = w(x) \quad (1)$$

The displacement of any point in the body along the x -direction is denoted by u_1 , along the y -direction by u_2 and along the z -direction by u_3 . Accordingly, the only nonzero strain is the axial strain ε_{xx} , which represents the axial elongation:

$$\varepsilon_{xx} = \frac{\partial u_1}{\partial x} = \frac{du}{dx} - z \frac{d^2w}{dx^2} \quad (2)$$

The axial force is calculated from the equation

$$N(x) = \int_A \sigma_{xx} dA \quad (3)$$

where σ_{xx} represents the normal stress and A denotes the cross-sectional area. For a homogeneous material, if the linear elastic constitutive relations are employed and Equation (2) is utilized, the following relation is obtained:

$$\sigma_{xx}(x, z) = E \varepsilon_{xx}(x, z) = E \left(\frac{du}{dx} - z \frac{d^2w}{dx^2} \right) \quad (4)$$

where E is the modulus of elasticity. Substituting Equation (4) into (3) yields

$$N(x) = \int_A \sigma_{xx} dA = \int_A E \left(\frac{du}{dx} - z \frac{d^2w}{dx^2} \right) dA = E \frac{du}{dx} \int_A dA - E \frac{d^2w}{dx^2} \int_A z dA = EA \frac{du}{dx} \quad (5)$$

The terms E , du/dx and d^2w/dx^2 are functions of x only and are therefore constant across the cross-section area A , allowing them to be moved outside the integrals. Furthermore, because the x -axis is defined as the centroidal axis of the cross-section, the first moment of area, $\int_A z dA$, is zero.

The equation of motion is derived using Hamilton's principle. Since only axial free vibration is considered—and apart from the support reactions, no external force acts on the beam—Hamilton's principle (Reddy, 2002) can be expressed as

$$\int_{t_1}^{t_2} (\delta K - \delta U) dt = 0 \quad (6)$$

Here, t denotes time, δ represents the variational operator, K is the kinetic energy and U is the strain energy. For this problem, the kinetic and strain energies are given by Equations (7) and (8), respectively, where ρ represents the mass density.

$$K = \frac{1}{2} \int_0^L \rho A \left(\frac{\partial u}{\partial t} \right)^2 dx \quad (7)$$

$$U = \frac{1}{2} \int_0^L EA \left(\frac{\partial u}{\partial x} \right)^2 dx + \frac{1}{2} k[u(0, t)]^2 \tag{8}$$

Substituting Equations (7) and (8) into (6) yields the expression for the motion.

$$0 = \int_{t_1}^{t_2} \left[\int_0^L \left(\rho A \frac{\partial u}{\partial t} \frac{\partial \delta u}{\partial t} - EA \frac{\partial u}{\partial x} \frac{\partial \delta u}{\partial x} \right) dx - ku(0, t) \delta u(0, t) \right] dt \tag{9}$$

In Equation (9) upon applying integration by parts to the first term of the integrand for the time variable, the following relation is obtained:

$$0 = \int_{t_1}^{t_2} \left[\int_0^L \left(-\rho A \frac{\partial^2 u}{\partial t^2} \delta u - EA \frac{\partial u}{\partial x} \frac{\partial \delta u}{\partial x} \right) dx - ku(0, t) \delta u(0, t) \right] dt \tag{10}$$

The axial displacement function for the vibration motion is chosen as

$$u(x, t) = u_0(x) e^{i\omega t} \tag{11}$$

which ensures the periodicity of the motion. In Equation (11) i denotes the imaginary unit, ω is the natural vibration frequency and $u_0(x)$ represents the vibration mode shape. Substituting Equation (11) into (10) and employing the equality $i^2 = -1$ leads to the relation:

$$0 = \int_{t_1}^{t_2} e^{2i\omega t} \left[\int_0^L \left(\rho A \omega^2 u_0 \delta u_0 - EA \frac{du_0}{dx} \frac{d\delta u_0}{dx} \right) dx - ku_0(0) \delta u_0(0) \right] dt \tag{12}$$

Since

$$\int_{t_1}^{t_2} e^{2i\omega t} dt \neq 0 \tag{13}$$

then

$$\int_0^L \left(\rho A \omega^2 u_0 \delta u_0 - EA \frac{du_0}{dx} \frac{d\delta u_0}{dx} \right) dx - ku_0(0) \delta u_0(0) = 0 \tag{14}$$

Applying integration by parts to the second term of the integrand in Equation (14) yields

$$\int_0^L \left(\rho A \omega^2 u_0 + EA \frac{d^2 u_0}{dx^2} \right) \delta u_0 dx - \left(ku_0(0) - EA \frac{du_0}{dx} \Big|_{x=0} \right) \delta u_0(0) = 0 \tag{15}$$

In Equation (15) because δu_0 and $\delta u_0(0)$ may assume arbitrary values, the coefficients of these terms must vanish; that is, they must equal zero:

$$\rho A \omega^2 u_0 + EA \frac{d^2 u_0}{dx^2} = 0, \quad 0 < x < L \tag{16}$$

$$ku_0(0) - EA \left. \frac{du_0}{dx} \right|_{x=0} = 0 \quad (17)$$

Equation (16) is the governing equation for the problem, while Equation (17) is the mixed boundary condition at the left end. As shown in Figure 1, the right end of the beam is a fixed support, which imposes the essential boundary condition that displacement must be zero:

$$u_0(L) = 0 \quad (18)$$

2.3. Non-dimensionalization

To non-dimensionalize the governing equation and boundary conditions, the following dimensionless variables and constants are defined:

$$\xi = \frac{x}{L}, \quad v = \frac{u_0}{L}, \quad \beta = \frac{kL}{EA}, \quad \eta = \frac{\rho L^2}{E} \omega^2 \quad (19)$$

Here, ξ is the dimensionless coordinate, v is the dimensionless displacement amplitude, β is the dimensionless stiffness ratio representing the spring's stiffness relative to the beam's axial stiffness and η is the dimensionless frequency parameter. When the dimensionless variables given in Equation (19) are substituted into Equation (16) the non-dimensional governing equation is obtained:

$$\frac{d^2v}{d\xi^2} + \eta v = 0, \quad 0 < \xi < 1 \quad (20)$$

Similarly, when the dimensionless variables and constants defined in Equation (19) are substituted into Equations (17) and (18) the non-dimensional boundary condition expressions are obtained:

$$\beta v(0) - \left. \frac{dv}{d\xi} \right|_{\xi=0} = 0 \quad (21)$$

$$v(1) = 0 \quad (22)$$

A key advantage of this formulation is the reduction of the parametric space; the problem is now defined by two dimensionless parameters (η and β) instead of the initial five physical parameters ρ, ω, E, A, L .

2.4. Analytical Solution of the Governing Equation

For the solution of Equation (20)

$$v(\xi) = e^{\lambda\xi} \quad (23)$$

is assumed. When Equation (23) is substituted into Equation (20) the following expression is obtained:

$$\frac{d^2}{d\xi^2}(e^{\lambda\xi}) + \eta e^{\lambda\xi} = \lambda^2 e^{\lambda\xi} + \eta e^{\lambda\xi} = (\lambda^2 + \eta)e^{\lambda\xi} = 0 \quad (24)$$

Since $e^{\lambda\xi} > 0$ for all $\lambda\xi$ values, it must be that

$$\lambda^2 + \eta = 0 \quad (25)$$

Equation (25) is a second-order polynomial dependent on λ , whose roots are given by:

$$\lambda_1 = i\sqrt{\eta}, \quad \lambda_2 = -i\sqrt{\eta} \quad (26)$$

Because Equation (20) is a homogeneous, linear differential equation, the principle of superposition applies. By employing this principle, the solution is obtained in the form

$$v(\xi) = c_1 e^{i\sqrt{\eta}\xi} + c_2 e^{-i\sqrt{\eta}\xi} \quad (27)$$

Substituting the Euler identity

$$e^{a+ib} = e^a(\cos(b) + i \sin(b)) \quad (28)$$

into Equation (27) yields the solution in the form

$$v(\xi) = c_1(\cos(\sqrt{\eta}\xi) + i \sin(\sqrt{\eta}\xi)) + c_2(\cos(\sqrt{\eta}\xi) - i \sin(\sqrt{\eta}\xi)) \quad (29)$$

Since c_1 and c_2 may be complex numbers, they can be expressed as $c_1 = a_1 + ib_1$ and $c_2 = a_2 + ib_2$, where a_1, a_2, b_1 and b_2 are real numbers. Rearranging Equation (29) using these values yields

$$v(\xi) = (c_1 + c_2) \cos(\sqrt{\eta}\xi) + i(c_1 - c_2) \sin(\sqrt{\eta}\xi) = (a_1 + a_2) \cos(\sqrt{\eta}\xi) + i(b_1 + b_2) \cos(\sqrt{\eta}\xi) - (b_1 - b_2) \sin(\sqrt{\eta}\xi) + i(a_1 - a_2) \sin(\sqrt{\eta}\xi) \quad (30)$$

For the solution to be real, it is necessary that $b_1 + b_2 = 0$ and $a_1 - a_2 = 0$. Hence, one may set $b_1 = -b_2 = b$ and $a_1 = a_2 = a$. In this case, Equation (30) becomes

$$v(\xi) = 2a \cos(\sqrt{\eta}\xi) - 2b \sin(\sqrt{\eta}\xi) \quad (31)$$

and, with $C = 2a$, $D = -2b$, it can be expressed as

$$v(\xi) = C \cos(\sqrt{\eta}\xi) + D \sin(\sqrt{\eta}\xi) \quad (32)$$

From the boundary condition given in Equation (21) the following expression is obtained:

$$\beta C - D\sqrt{\eta} = 0, \quad (33)$$

and from the boundary condition in Equation (22):

$$C \cos(\sqrt{\eta}) + D \sin(\sqrt{\eta}) = 0 \quad (34)$$

From Equation (33) one obtains $C/D = \sqrt{\eta}/\beta$ and from Equation (34) one obtains $C/D = -\tan(\sqrt{\eta})$. Equating and rearranging these two values leads to the transcendental equation

$$\frac{\sqrt{\eta}}{\beta} + \tan(\sqrt{\eta}) = 0 \quad (35)$$

Once the roots for η from Equation (35) are determined, the vibration frequencies can be obtained by using the relation $\omega^2 = \eta E/(\rho L^2)$ provided in Equation (19).

2.5. Ritz method formulation

In the Ritz method, an approximate solution $V_N(\xi)$ is sought in the form:

$$v(\xi) \approx V_N(\xi) = \phi_0 + \sum_{i=1}^N c_i \phi_i(\xi) \quad (36)$$

where ϕ_0 and ϕ_i are the approximation functions and c_i are the unknown real parameters to be determined for $i = 1, 2, \dots, N$. N , must be specified before commencing the calculations. The approximation function ϕ_0 must satisfy the prescribed essential boundary conditions; since only condition Equation (22) represents an essential boundary condition and its value is zero, ϕ_0 is chosen as $\phi_0 = 0$. The approximation functions $\phi_i (i = 1, 2, \dots, N)$ must satisfy the homogeneous form of the prescribed essential boundary conditions.

The approximation functions are selected as

$$\phi_i(\xi) = 1 - \xi^i, (i = 1, 2, \dots, N) \quad (37)$$

When the dimensionless parameters defined in Equation (19) are used in Equation (14) one obtains

$$\int_0^1 \left(\eta v \delta v - \frac{dv}{d\xi} \frac{d\delta v}{d\xi} \right) d\xi - \beta v(0) \delta v(0) = 0 \tag{38}$$

In Equation (38) by expressing $v(\xi)$ as

$$v(\xi) = \sum_{j=1}^N c_j \phi_j(\xi) \tag{39}$$

and for the virtual displacement using

$$\delta v = \sum_{i=1}^N \delta c_i \phi_i(\xi) \tag{40}$$

one obtains

$$\sum_{i=1}^N \delta c_i \left\{ \sum_{j=1}^N c_j \left[\eta \int_0^1 \phi_i \phi_j d\xi - \left(\int_0^1 \frac{d\phi_i}{d\xi} \frac{d\phi_j}{d\xi} d\xi + \beta \phi_i(0) \phi_j(0) \right) \right] \right\} = 0 \tag{41}$$

Since the variations $\delta c_i (i = 1, 2, \dots, N)$ are arbitrary and independent, the coefficients of δc_i must vanish, yielding

$$\sum_{j=1}^N \left[\eta \int_0^1 \phi_i \phi_j d\xi - \left(\int_0^1 \frac{d\phi_i}{d\xi} \frac{d\phi_j}{d\xi} d\xi + \beta \phi_i(0) \phi_j(0) \right) \right] c_j = 0 \tag{42}$$

Thus, an N -linear equation system in N unknowns are obtained. Solving this linear system yields the coefficients $c_j (j = 1, 2, \dots, N)$. Multiplying Equation (42) by -1 , it can be written in matrix form as

$$(\mathbf{A} - \eta \mathbf{M}) \mathbf{c} = \mathbf{0} \tag{43}$$

where the matrix elements are defined by

$$A_{ij} = \int_0^1 \frac{d\phi_i}{d\xi} \frac{d\phi_j}{d\xi} d\xi + \beta \phi_i(0) \phi_j(0) \tag{44}$$

$$M_{ij} = \int_0^1 \phi_i \phi_j d\xi \tag{45}$$

and using these equations, the matrices \mathbf{A} and \mathbf{M} are constructed.

3. Ritz Method Solution

It should be noted that a key advantage of the non-dimensional formulation is that the results for the dimensionless natural frequency ($\bar{\omega}$) are independent of the specific material (E, ρ) and geometric (A, L) parameters. The solution depends solely on the dimensionless stiffness ratio β . For the numerical examples presented in this study, a value of $\beta = 2$ was chosen. This value represents a physically meaningful case where the spring stiffness is of the same order of magnitude as the beam's axial stiffness. It should be emphasized that the primary focus of this work is to demonstrate the rapid convergence of the Ritz method to the analytical solution. This convergence property is independent of the specific value chosen for β ; the selected value simply provides a representative, non-trivial elastic boundary condition to effectively test the method's accuracy.

In the approximate solution Equation (36) when N parameters are employed, N frequencies can be computed. In addition, the calculations are performed for the dimensionless natural frequency, $\bar{\omega}$, defined by

$$\bar{\omega} = \omega(L\sqrt{\rho/E}) = \sqrt{\eta} \quad (46)$$

The first eight frequency values obtained from the analytical solution and the Ritz method are compared. The “exact” dimensionless natural frequencies listed in the tables were calculated by first numerically determining the roots of the transcendental equation (35) using the Newton-Raphson method and then taking the square root of each resulting root (η). The graph of the function $\sqrt{\eta}/\beta + \tan(\sqrt{\eta})$ from Equation (35) is presented in Figure 2.

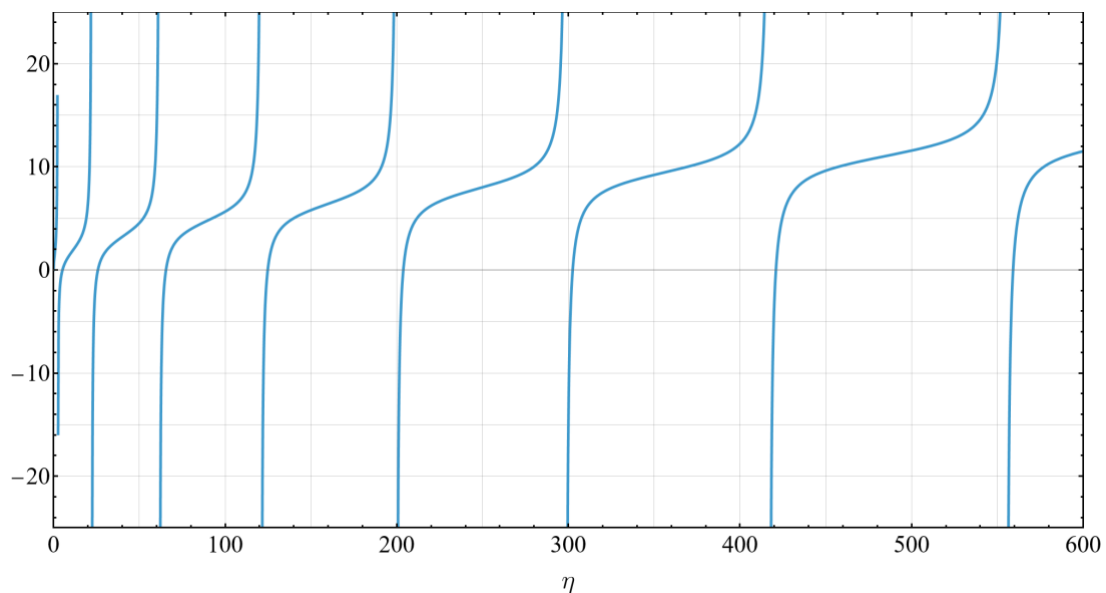


Figure 2. Graph of the function $\sqrt{\eta}/\beta + \tan(\sqrt{\eta})$ from Equation (35) for $\beta = 2$.

Figure 2 illustrates the graphical solution to the transcendental equation (35) for the case where the stiffness ratio is $\beta = 2$. The horizontal axis represents the dimensionless frequency parameter η , while the vertical axis shows the value of the function. The points where the curve intersects the horizontal axis (i.e., where the function equals zero) are the roots of the equation. These roots represent the specific values of η and their square roots provide the dimensionless natural frequencies ($\bar{\omega}$) of the beam.

In Equation (43) for the coefficients $c_j (j = 1, 2, \dots, N)$ to acquire nontrivial values, the values of η are determined from the roots of the characteristic polynomial, which is obtained by setting the determinant of the coefficient matrix $(\mathbf{A} - \eta\mathbf{M})$ equal to zero. When the approximation functions given in Equation (37) are used in Equations (44) and (45), the following matrices are obtained:

For $N = 1$:

$$\mathbf{A} = [3], \quad \mathbf{M} = [1/3] \quad (47)$$

For $N = 2$:

$$\mathbf{A} = \begin{bmatrix} 3 & 3 \\ 3 & 10/3 \end{bmatrix}, \quad \mathbf{M} = \begin{bmatrix} 1/3 & 5/12 \\ 5/12 & 8/15 \end{bmatrix} \quad (48)$$

For $N = 3$:

$$\mathbf{A} = \begin{bmatrix} 3 & 3 & 3 \\ 3 & 10/3 & 7/2 \\ 3 & 7/2 & 19/5 \end{bmatrix}, \quad \mathbf{M} = \begin{bmatrix} 1/3 & 5/12 & 9/20 \\ 5/12 & 8/15 & 7/12 \\ 9/20 & 7/12 & 9/14 \end{bmatrix} \quad (49)$$

Examination of Equations (47) - (49) reveals that, as the number of parameters increases, the previously computed elements remain unchanged; thus, only the computation of the new elements is necessary. This property is a general characteristic of the Ritz method, evident from Equations (44) and (45). The results obtained from both the Ritz method and the analytical solution are presented in Table 1.

Table 1. The first eight dimensionless natural frequencies, $\bar{\omega}$, obtained from the Ritz method and the analytical solution ($\beta = 2$).

N	$\bar{\omega}_1$	$\bar{\omega}_2$	$\bar{\omega}_3$	$\bar{\omega}_4$	$\bar{\omega}_5$	$\bar{\omega}_6$	$\bar{\omega}_7$	$\bar{\omega}_8$
1	3.0000							
2	2.2998	6.7363						
3	2.2907	5.2120	11.5147					
4	2.2889	5.1142	8.5647	17.4141				
5	2.2889	5.0880	8.2220	12.3362	24.5104			
6	2.2889	5.0871	8.1083	11.5305	16.6009	32.8420		
7	2.2889	5.0870	8.0980	11.2310	15.0655	21.4281	42.4269	
8	2.2889	5.0870	8.0963	11.1849	14.4547	18.8810	26.8587	53.2736
Exact	2.2889	5.0870	8.0962	11.1727	14.2764	17.3932	20.5175	23.6463

Inspection of Table 1 shows that, as the number of parameters increases, the corresponding frequency values rapidly converge to those obtained from the analytical solution. In Table 2, the first eight dimensionless natural frequencies are presented for the case where $N = 19$ is taken in the Ritz method and is compared with the analytical solution.

Table 2. The first eight dimensionless natural frequencies, $\bar{\omega}$, obtained using 19 parameters in the Ritz method and from the analytical solution ($\beta = 2$).

N	$\bar{\omega}_1$	$\bar{\omega}_2$	$\bar{\omega}_3$	$\bar{\omega}_4$	$\bar{\omega}_5$	$\bar{\omega}_6$	$\bar{\omega}_7$	$\bar{\omega}_8$
Ritz	2.2889	5.0870	8.0962	11.1727	14.2764	17.3932	20.5175	23.6463
Exact	2.2889	5.0870	8.0962	11.1727	14.2764	17.3932	20.5175	23.6463

Examination of Table 2 indicates that the analytical and Ritz solutions agree to 5 (6) significant digits.

4. Conclusions

Numerical methods based on variational approximation methods are the most effective numerical methods in solid mechanics. Since the approximation functions used in the approximate solution are the basis vectors of the solution vector space, the approximate solution approaches the analytical solution as the number of parameters, N , increases. When numerical rounding and truncation errors are ignored, the absolute value of the difference between the analytical solution and the approximate solution can be ensured to remain below any positive value selected by increasing the number of parameters.

There are many variational approximation methods. Galerkin method, least squares method, collocation method and subregion method are some of these methods. It is not mandatory to use

polynomials as approximation functions. If desired, trigonometric functions or functions that satisfy the continuity conditions of the problem can be used. Polynomials are often selected as approximation functions because they facilitate integration and differentiation operations.

Variational approximation methods give satisfactory results not only in beam problems but also in problems where plates, shells and three-dimensional objects are examined. The disadvantage of these methods is that it becomes challenging to determine approximation functions when the geometry and boundary conditions of the problem become complex.

The Ritz method used in the study simplifies the selection of approximation functions compared to other variational approximation methods, as it weakens the continuity conditions that the solution of the governing equation must satisfy. When the obtained results are examined, it is observed that the approximate solution converges quite quickly to the analytical solution.

The Ritz method stands out as a highly effective alternative solution in cases where an analytical solution is complicated or nonexistent due to its features, such as its ability to be applied to different types of problems, the systematic derivation of its formulation, and high convergence speed. While an analytical solution was available for the uniform, spring-supported beam studied here, many practical engineering structures feature non-uniform cross-sections or functionally graded materials for which such exact solutions are intractable. The demonstrated high accuracy and rapid convergence of the Ritz method for this benchmark problem confirm its role as a powerful and reliable tool for engineers to accurately predict the vibrational behavior of these more complex, real-world structural systems.

Authors' Contributions

All authors contributed equally to the study.

Statement of Conflicts of Interest

There is no conflict of interest between the authors.

Statement of Research and Publication Ethics

The author declares that this study complies with Research and Publication Ethics.

References

- Akgöz, B. (2019). Ritz yöntemi ile değişken kesitli kolonların burkulma analizi. *Mühendislik Bilimleri ve Tasarım Dergisi*, 7(2), 452–458. <https://doi.org/10.21923/jesd.539288>
- Akgöz, B., and Civalek, Ö. (2012). Longitudinal vibration analysis for microbars based on strain gradient elasticity theory. *Journal of Vibration and Control*, 20(4), 606–616. <https://doi.org/10.1177/1077546312463752>
- Akgöz, B., and Civalek, Ö. (2022). Buckling Analysis of Functionally Graded Tapered Microbeams via Rayleigh–Ritz Method. *Mathematics*, 10(23), 4429. <https://doi.org/10.3390/math10234429>
- Bhat, R. B. (1985). Natural frequencies of rectangular plates using characteristic orthogonal polynomials in Rayleigh–Ritz method. *Journal of Sound and Vibration*, 102(4), 493–499. [https://doi.org/10.1016/S0022-460X\(85\)80109-7](https://doi.org/10.1016/S0022-460X(85)80109-7)
- Bhat, R. B. (1986). Transverse vibrations of a rotating uniform cantilever beam with tip mass as predicted by using beam characteristic orthogonal polynomials in the Rayleigh–Ritz method. *Journal of Sound and Vibration*, 105(2), 199–210. [https://doi.org/10.1016/0022-460X\(86\)90149-5](https://doi.org/10.1016/0022-460X(86)90149-5)
- Blevins, R. D. (1974). Fluid Elastic Whirling of a Tube Row. *Journal of Pressure Vessel Technology*, 96(4), 263–267. <https://doi.org/10.1115/1.3454179>
- Carrera, E. (1998). Evaluation of Layerwise Mixed Theories for Laminated Plates Analysis. *AIAA Journal*, 36(5), 830–839. <https://doi.org/10.2514/2.444>
- Chakraverty, S., and Behera, L. (2014). Free vibration of rectangular nanoplates using Rayleigh–Ritz method. *Physica E: Low-Dimensional Systems and Nanostructures*, 56, 357–363. <https://doi.org/10.1016/j.physe.2013.08.014>
- Challamel, N., & Zingales, M. (2025). Two-Phase Peridynamic Elasticity with Exponential Kernels. I: Statics and Vibrations of Axial Rods. *Journal of Engineering Mechanics*, 151(5). <https://doi.org/10.1061/JENMDT.EMENG-8252>
- Civalek, Ö., Uzun, B., and Yaylı, M. Ö. (2020). Stability analysis of nanobeams placed in electromagnetic field using a finite element method. *Arabian Journal of Geosciences*, 13, 1165. <https://doi.org/10.1007/S12517-020-06188-8>
- Civalek, Ö., Uzun, B., and Yaylı, M. Ö. (2022a). A Fourier sine series solution of static and dynamic response of nano/micro micro-scaled FG rod under torsional effect. *Advances in Nano Research*, 12(5), 467 – 482. <https://doi.org/10.12989/anr.2022.12.5.467>
- Civalek, Ö., Uzun, B., and Yaylı, M. Ö. (2022b). Nonlocal Free Vibration of Embedded Short-Fiber-Reinforced Nano-/Micro-Rods with Deformable Boundary Conditions. *Materials*, 15(19), 6803. <https://doi.org/10.3390/ma15196803>
- Dos Santos, J. V. A., and Reddy, J. N. (2012). Free vibration and buckling analysis of beams with a modified couple-stress theory. *International Journal of Applied Mechanics*, 4(3), 1250026. <https://doi.org/10.1142/S1758825112500263>
- Elliott, A. J., and Cammarano, A. (2024). Incorporating Boundary Nonlinearity into Structural Vibration Problems. *Vibration*, 7(4), 949–969. <https://doi.org/10.3390/vibration7040050>
- Gantayat, A. K., Sutar, M. K., Mohanty, J. R., and Pattnaik, S. (2024). Free vibration analysis of an O-pattern graphene reinforced axial functionally graded polymer matrix nano-composite non-uniform beam. *Journal of Elastomers & Plastics*, 56(7), 897–906. <https://doi.org/10.1177/00952443241281986>
- Gao, C., Pang, F., Li, H., Wang, H., Cui, J., and Huang, J. (2021). Free and Forced Vibration Characteristics Analysis of a Multispan Timoshenko Beam Based on the Ritz Method. *Shock and Vibration*, 4440250. <https://doi.org/10.1155/2021/4440250>
- Inman, D. J. (2017). *Vibration with Control*. Hoboken, NJ: John Wiley & Sons. <https://doi.org/10.1002/9781119375081>
- Kafkas, U. (2024). On the free vibration of a perforated Rayleigh beam with deformable ends. *Engineering Science and Technology, an International Journal*, 56, 101787. <https://doi.org/10.1016/J.JESTCH.2024.101787>
- Kong, S., Zhou, S., Nie, Z., and Wang, K. (2008). The size-dependent natural frequency of Bernoulli–Euler micro-beams. *International Journal of Engineering Science*, 46(5), 427–437. <https://doi.org/10.1016/j.ijengsci.2007.10.002>
- Laura, P. A. A., Ercoli, L., Grossi, R. O., Nagaya, K., and Sarmiento, G. S. (1985). Transverse vibrations of composite membranes of arbitrary boundary shape. *Journal of Sound and Vibration*, 101(3), 299–306. [https://doi.org/10.1016/S0022-460X\(85\)80130-9](https://doi.org/10.1016/S0022-460X(85)80130-9)

- Lee, J. W. (2023). Free Vibration Analysis of Elastically Restrained Tapered Beams with Concentrated Mass and Axial Force. *Applied Sciences*, 13(19), 10742. <https://doi.org/10.3390/app131910742>
- Leissa, A. W. (2005). The historical bases of the Rayleigh and Ritz methods. *Journal of Sound and Vibration*, 287(4), 961–978. <https://doi.org/10.1016/j.jsv.2004.12.021>
- Li, L., Hu, Y., and Li, X. (2016). Longitudinal vibration of size-dependent rods via nonlocal strain gradient theory. *International Journal of Mechanical Sciences*, 115–116, 135–144. <https://doi.org/10.1016/j.ijmecsci.2016.06.011>
- Li, Z., Lin, B., Chen, B., Zhao, X., and Li, Y. (2022). Free Vibration, Buckling and Dynamical Stability of Timoshenko Micro/Nano-Beam Supported on Winkler-Pasternak Foundation Under a Follower Axial Load. *International Journal of Structural Stability and Dynamics*, 22(9), 2250113. <https://doi.org/10.1142/S0219455422501139>
- Mazanoglu, K. (2017). Natural frequency analyses of segmented Timoshenko–Euler beams using the Rayleigh–Ritz method. *Journal of Vibration and Control*, 23(13), 2135–2154. <https://doi.org/10.1177/1077546315611525>
- Mirzajani, M., Khaji, N., and Hori, M. (2018). Stress Wave Propagation Analysis in One-Dimensional Micropolar Rods with Variable Cross-Section Using Micropolar Wave Finite Element Method. *International Journal of Applied Mechanics*, 10(4), 1850039. <https://doi.org/10.1142/S1758825118500394>
- Modak, K., Saravanan, T. J., and Rajasekharan, S. (2024). Dynamic Analysis of Coupled Axial-Bending Wave Propagation in a Cracked Timoshenko Beam Using Spectral Finite-Element Method. *Journal of Vibration Engineering & Technologies*, 12, 1225–1247. <https://doi.org/10.1007/s42417-023-00903-x>
- Nazemnezhad, R., & Shokrollahi, H. (2020). Free axial vibration of cracked axially functionally graded nanoscale rods incorporating surface effect. *Steel and Composite Structures*, 35(3), 449–462. <https://doi.org/10.12989/SCS.2020.35.3.449>
- Nejadsadeghi, N., and Misra, A. (2021). On the statics and dynamics of granular-microstructured rods with higher order effects. *Mathematics and Mechanics of Solids*, 26(12), 1815–1837. <https://doi.org/10.1177/10812865211009938>
- Oguaghamba, O. A., Ike, C. C., Ikwueze, E. U., and Ofondu, I. O. (2023). Ritz Variational Method for Solving the Elastic Buckling Problems of Thin-Walled Beams with Bisymmetric Cross-Sections. *Mathematical Modelling of Engineering Problems*, 10(1), 129–138. <https://doi.org/10.18280/mmep.100114>
- Pei, Z. (2024). Free vibration Analysis of Beams with Functional Gradient Materials with Cracks. *Academic Journal of Science and Technology*, 11(1), 265–269. <https://doi.org/10.54097/eawe6q56>
- Pradhan, K. K., and Chakraverty, S. (2013). Free vibration of Euler and Timoshenko functionally graded beams by Rayleigh–Ritz method. *Composites Part B: Engineering*, 51, 175–184. <https://doi.org/10.1016/j.compositesb.2013.02.027>
- Rahbar-Ranji, A., and Shahbaztabar, A. (2017). Free vibration analysis of beams on a Pasternak foundation using Legendre polynomials and Rayleigh-Ritz method. *Odes'kyi Politechnichnyi Universytet Pratsi*, 3(53), 20–31. <https://doi.org/10.15276/opu.3.53.2017.03>
- Rahgozar, P. (2020). Free Vibration of Tall Buildings using Energy Method and Hamilton's Principle. *Civil Engineering Journal*, 6(5), 945–953. <https://doi.org/10.28991/cej-2020-03091519>
- Rao, S. S. (2007). *Vibration of continuous systems*. Hoboken, NJ: John Wiley & Sons.
- Rao, S. S. (2018). *Mechanical Vibrations* (6th ed.). Harlow, UK: Pearson.
- Reddy, J. N. (2007). Nonlocal theories for bending, buckling and vibration of beams. *International Journal of Engineering Science*, 45(2–8), 288–307. <https://doi.org/10.1016/J.IJENGSCI.2007.04.004>
- Reddy, J. N. (2017). *Energy principles and variational methods in applied mechanics* (3rd ed.). Hoboken, NJ: John Wiley & Sons.
- Reddy, J. N. (2022). *Theories and Analyses of Beams and Axisymmetric Circular Plates*. Boca Raton: CRC Press. <https://doi.org/10.1201/9781003240846>
- Ritz, W. (1909a). Theorie der Transversalschwingungen einer quadratischen Platte mit freien Rändern. *Annalen Der Physik*, 333(4), 737–786. <https://doi.org/10.1002/andp.19093330403>
- Ritz, W. (1909b). Über eine neue Methode zur Lösung gewisser Variationsprobleme der mathematischen Physik. *Journal Für Die Reine Und Angewandte Mathematik*, 1909(135), 1–61. <https://doi.org/10.1515/crll.1909.135.1>
- Senjanović, I., Alujević, N., Čatipović, I., Čakmak, D., and Vladimir, N. (2018). Vibration analysis of rotating toroidal shell by the Rayleigh-Ritz method and Fourier series. *Engineering Structures*, 173, 870–891. <https://doi.org/10.1016/j.engstruct.2018.07.029>

- Singh, P. P., and Azam, M. S. (2021). Free vibration and buckling analysis of elastically supported transversely inhomogeneous functionally graded nanoplate in thermal environment using Rayleigh–Ritz method. *Journal of Vibration and Control*, 27(23–24), 2835–2847. <https://doi.org/10.1177/1077546320966932>
- Soltani, D., Akbarzadeh Khorshidi, M., and Sedighi, H. M. (2021). Higher order and scale-dependent micro-inertia effect on the longitudinal dispersion based on the modified couple stress theory. *Journal of Computational Design and Engineering*, 8(1), 189–194. <https://doi.org/10.1093/jcde/qwaa070>
- Uzun, B., Civalek, Ö., and Yaylı, M. Ö. (2023a). A Hardening Nonlocal Elasticity Approach to Axial Vibration Analysis of an Arbitrarily Supported FG Nanorod. *Physical Mesomechanics*, 26(3), 295–312. <https://doi.org/10.1134/S1029959923030050>
- Uzun, B., Civalek, Ö., and Yaylı, M. Ö. (2023b). Vibration of FG nano-sized beams embedded in Winkler elastic foundation and with various boundary conditions. *Mechanics Based Design of Structures and Machines*, 51(1), 481–500. <https://doi.org/10.1080/15397734.2020.1846560>
- Uzun, B., Kafkas, U., and Yaylı, M. Ö. (2021). Free vibration analysis of nanotube based sensors including rotary inertia based on the Rayleigh beam and modified couple stress theories. *Microsystem Technologies*, 27(5), 1913–1923. <https://doi.org/10.1007/s00542-020-04961-z>
- Wang, S. (1997). A unified Timoshenko beam B-spline Rayleigh-Ritz method for vibration and buckling analysis of thick and thin beams and plates. *International Journal for Numerical Methods in Engineering*, 40(3), 473 – 491. [https://doi.org/10.1002/\(SICI\)1097-0207\(19970215\)40:3<473::AID-NME75>3.0.CO;2-U](https://doi.org/10.1002/(SICI)1097-0207(19970215)40:3<473::AID-NME75>3.0.CO;2-U)
- Warburton, G. B. (1979). Response using the Rayleigh-Ritz method. *Earthquake Engineering & Structural Dynamics*, 7(4), 327–334. <https://doi.org/10.1002/eqe.4290070404>
- Wu, J., Wang, J., Xie, L., Zhgoon, S., Wu, R., Zhang, A., ... Du, J. (2023). An analysis and experimental validation of natural frequencies of elastic ellipsoids with the Rayleigh–Ritz method. *Mechanics of Advanced Materials and Structures*, 30(17), 3491–3501. <https://doi.org/10.1080/15376494.2022.2077486>
- Xu, Y., and Wang, N. (2020). Transverse free vibration of Euler-Bernoulli beam with pre-axial pressure resting on a variable Pasternak elastic foundation under arbitrary boundary conditions. *Latin American Journal of Solids and Structures*, 17(7), e305. <https://doi.org/10.1590/1679-78256150>
- Yaylı, M. Ö. (2015). Buckling analysis of a rotationally restrained single walled carbon nanotube. *Acta Physica Polonica A*, 127(3), 678–683. <https://doi.org/10.12693/APhysPolA.127.678>
- Yıldırım, V. (2018). Some closed-form bending formulas for elastically restrained Euler-Bernoulli beams under point and uniformly distributed loads. *Journal of Applied Mathematics and Computational Mechanics*, 17(3), 97–109. <https://doi.org/10.17512/jamcm.2018.3.09>